Supporting Information

Large Scale and Controllable Synthesis of Graphene Quantum Dots from Rice Husk Biomass: A Comprehensive Utilization Strategy

Zhaofeng Wang,[a] Jingfang Yu,[b] Xin Zhang,[a,c] Na Li,[d] Bin Liu,[d] Yanyan Li,[e] Yuhua Wang,[e] Weixing Wang,[f] Yezhou Li,[a] Lichun Zhang,[a] Shanka Dissanayake,[g] Steven L. Suib,[a,g] Luyi Sun[a,b*]

[a]*Institute of Materials Science, University of Connecticut, Storrs, Connecticut 06269, United States*
[b]*Department of Chemical & Biomolecular Engineering, University of Connecticut, Storrs, Connecticut 06269, United States*
[c]*Department of Physics and Optoelectronic Engineering, Guangdong University of Technology, Guangzhou 510006, China*
[d]*School of Stomatology, Lanzhou University, Lanzhou, 730000, China*
[e]*Department of Materials Science, School of Physical Science and Technology, Lanzhou University, Lanzhou, 730000, China*
[f]*Ministry of Education Key Laboratory of Enhanced Heat Transfer & Energy Conservation, School of Chemistry and Chemical Engineering, South China University of Technology, Guangzhou, Guangdong 510640, China*
[g]*Department of Chemistry, University of Connecticut, Storrs, Connecticut 06269, United States*

* Corresponding author.

Dr. Luyi Sun, Tel: (860) 486-6895; Fax: (860) 486-4745; Email: luyi.sun@uconn.edu

1. Structural analysis of RHA and RHC

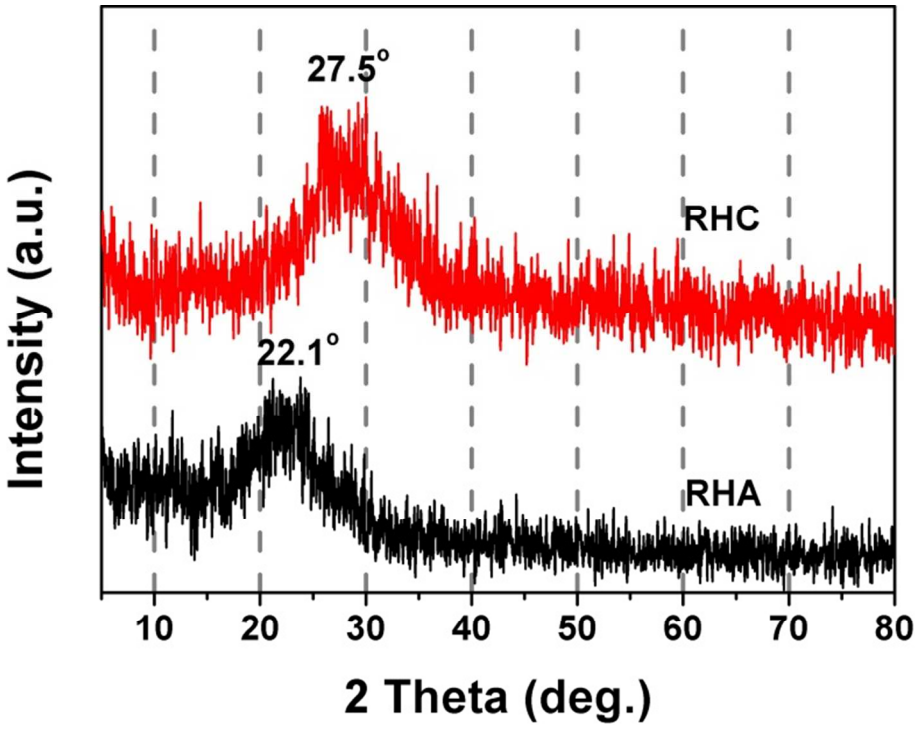

Figure S1. XRD patterns of the as-prepared RHA and RHC. RHA and RHC exhibit broad bands centered at ca. 22.1° and 27.5°, corresponding to the characteristic structures of amorphous silica and carbon, respectively. The evolution of the XRD patterns confirms that RHC was successfully extracted from RHA.

2. Morphology of RHC

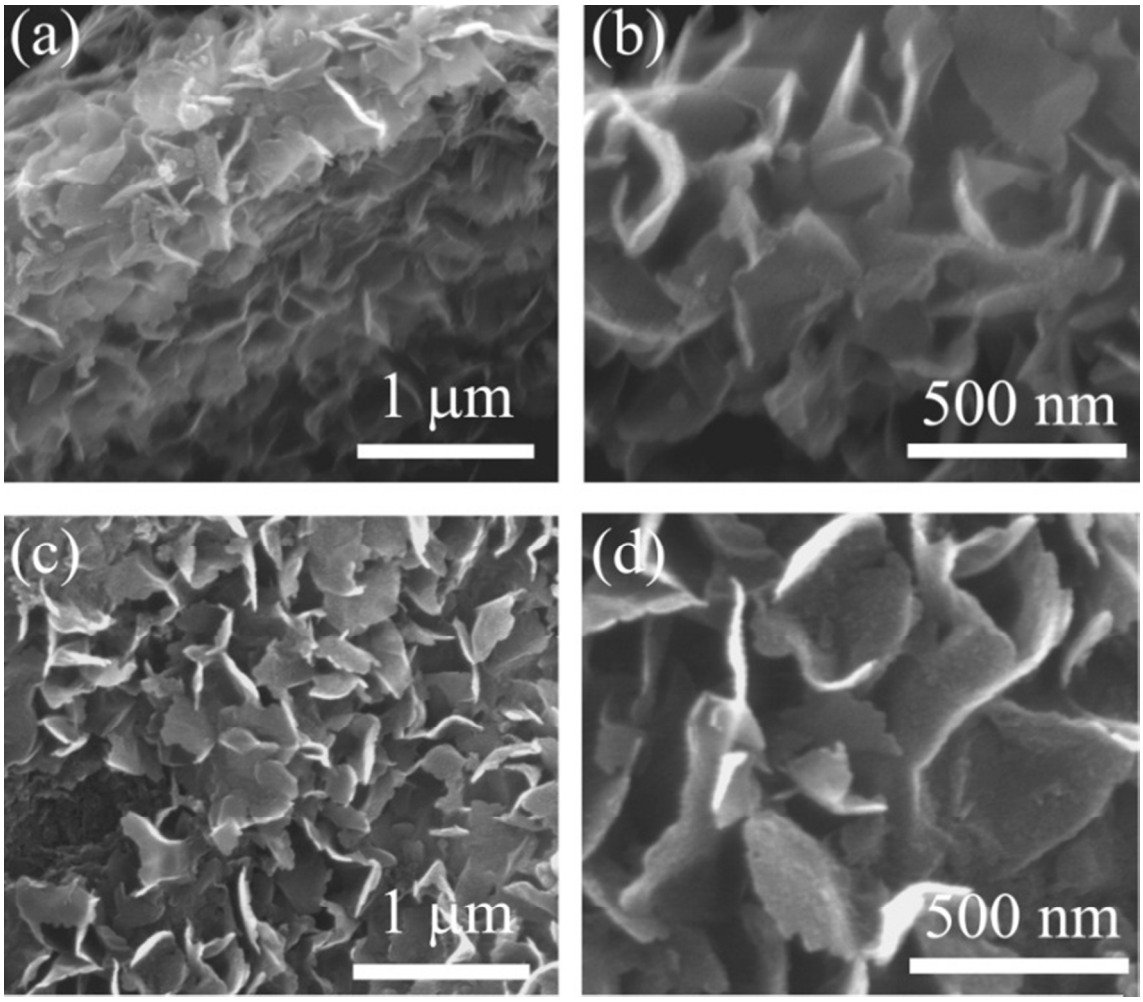

Figure S2. SEM micrographs of RHC (a, b) before and (c, d) after oxidation.

3. Characterization of silica from RH derived sodium silicate

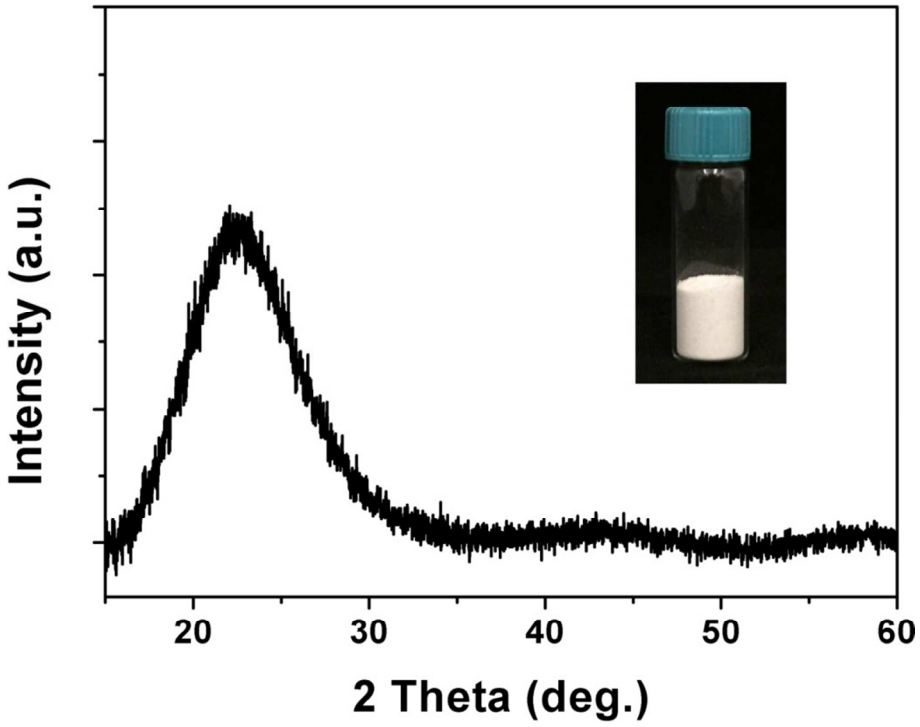

Figure S3. XRD pattern of the silica particles from RH derived sodium silicate; the inset shows the digital photograph of the as-prepared silica.

4. Chemical composition and structure of RH-GQDs

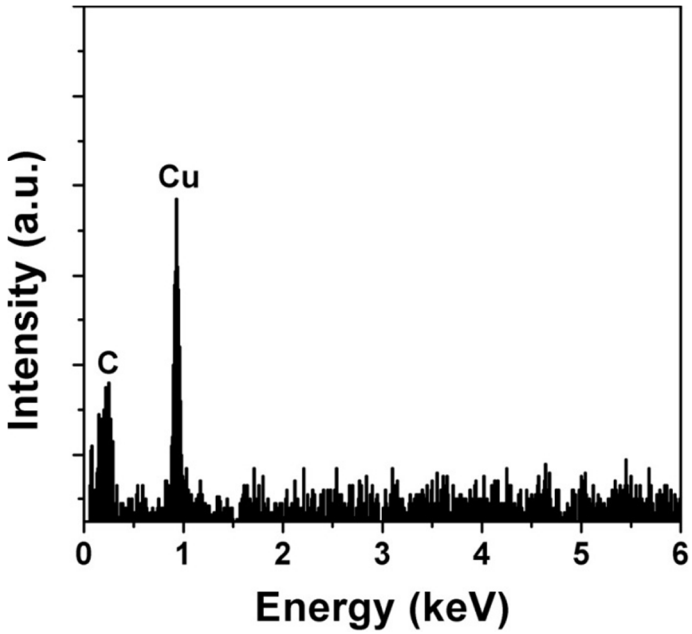

Figure S4. Energy-dispersive X-ray spectroscopy spectrum of the RH-GQDs synthesized at 200 °C.

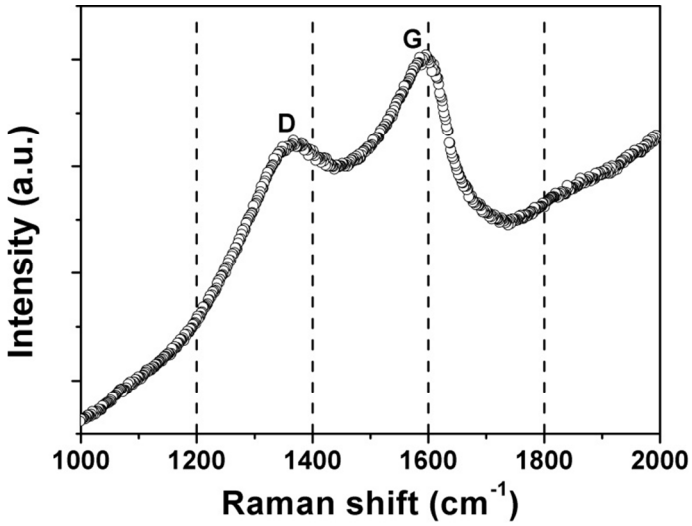

Figure S5. Raman spectrum of the RH-GQDs synthesized at 200 °C.

5. Quantum yield calculation

The photoluminescence quantum yield (QY) of the as-prepared RH-GQDs was calculated using Rhodamine B as a refernece dye based on the following equation:[1]

$$\eta_s = \eta_{ref} \times \frac{I_s \times \alpha_{ref} \times n_s^2}{I_{ref} \times \alpha_s \times n_{ref}^2}$$

where I, α, and n represent the integrated area of the PL emission, extinction coefficient at the excitation wavelength, and refractive index of the solvent, respectively, for the sample (*s*) and reference (*ref*).

6. PL behaviors

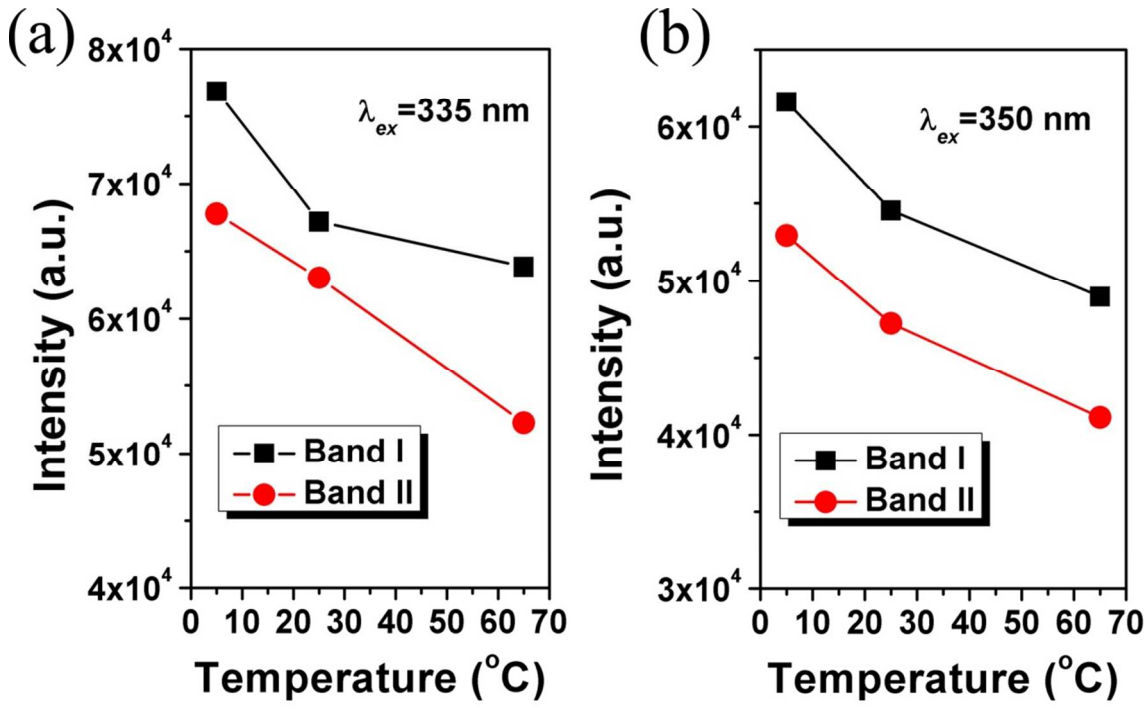

Figure S6. Temperature-dependent PL intensity of RH-GQDs excited by (a) 335 and (b) 350 nm.

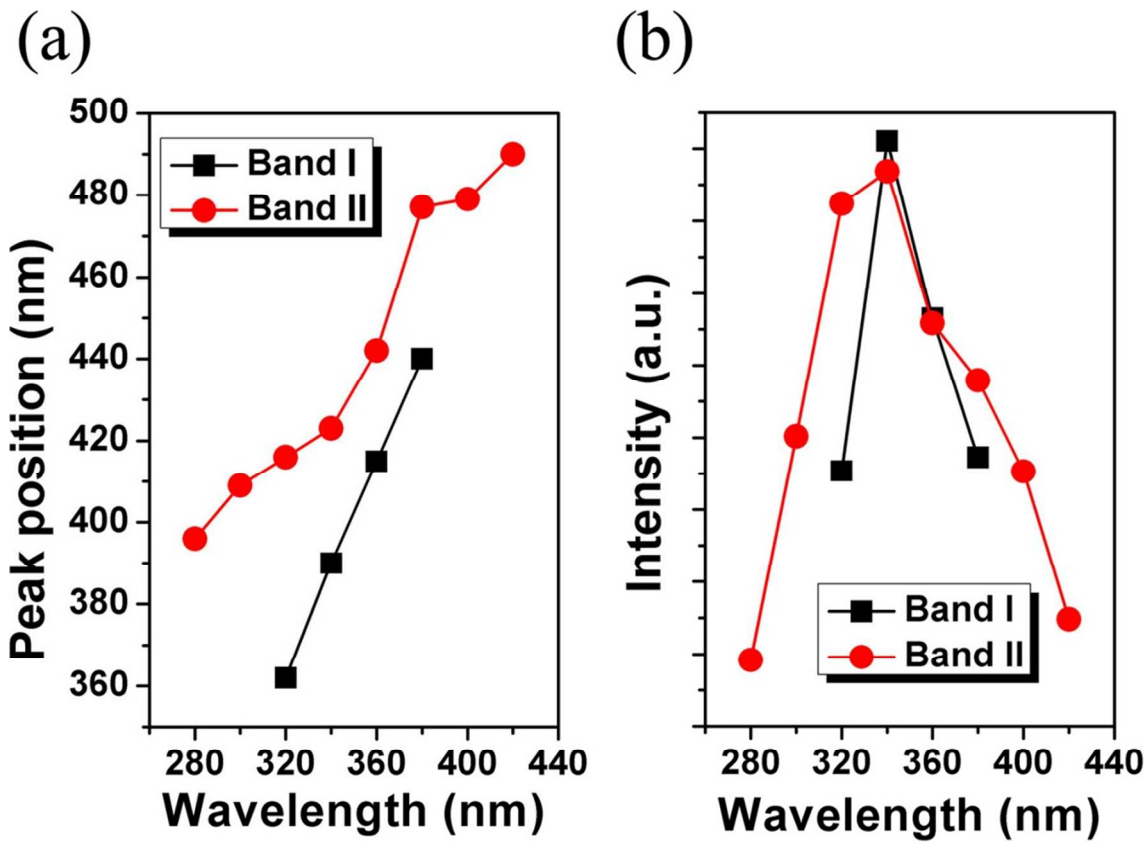

Figure S7. Excitation wavelength dependent PL of the RH-GQDs prepared at 200 °C: (a) peak position and (b) intensity.

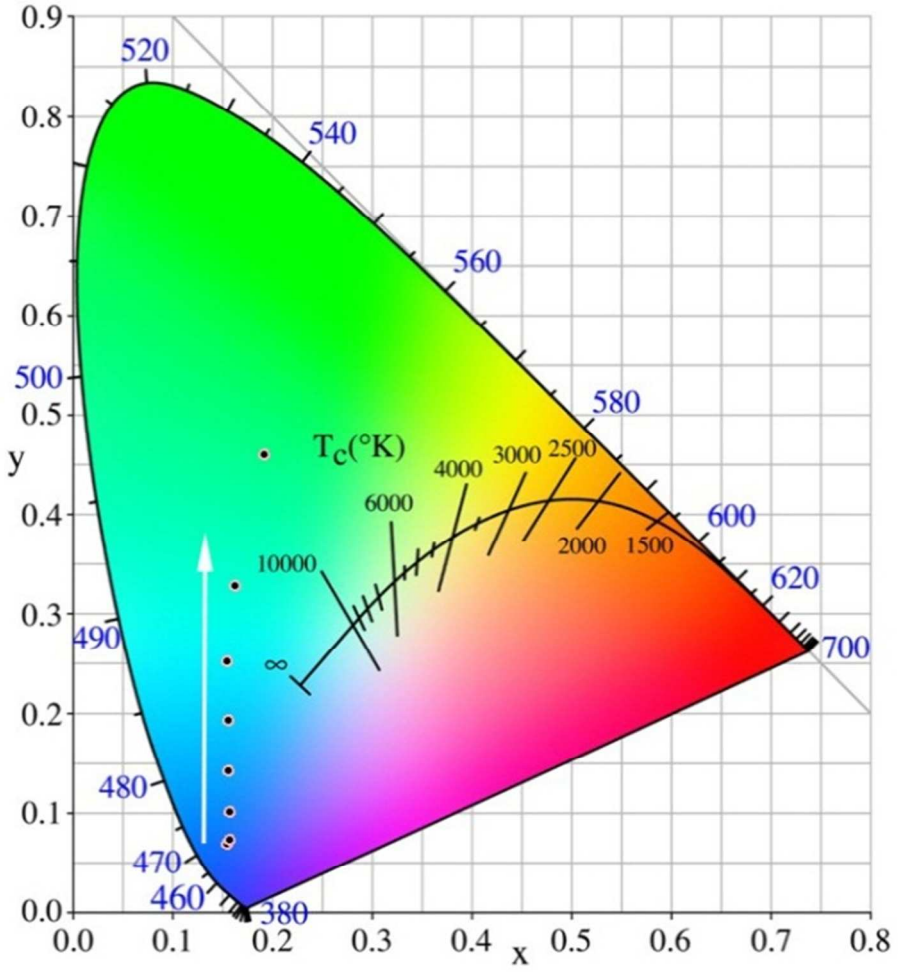

Figure S8. International commission on illumination (CIE) chromaticity diagram for RH-GQDs synthesized at 200 °C with excitation from 300 to 440 nm at 25 ºC. The black dots represent the corresponding color coordinates.

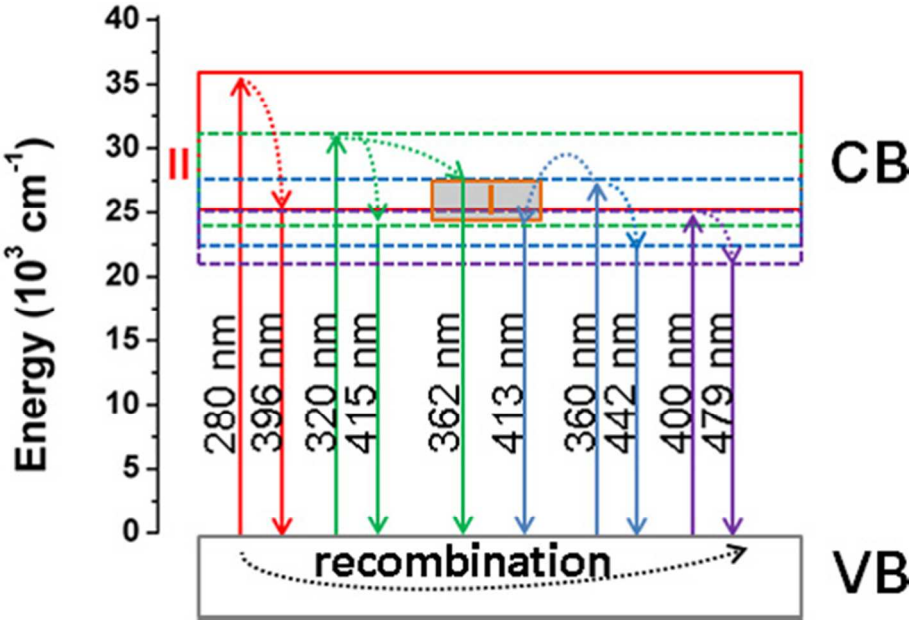

Figure S9. Proposed PL processes of the RH-GQDs based on the intrinsic and defect-related emissions.

7. Cell morphology

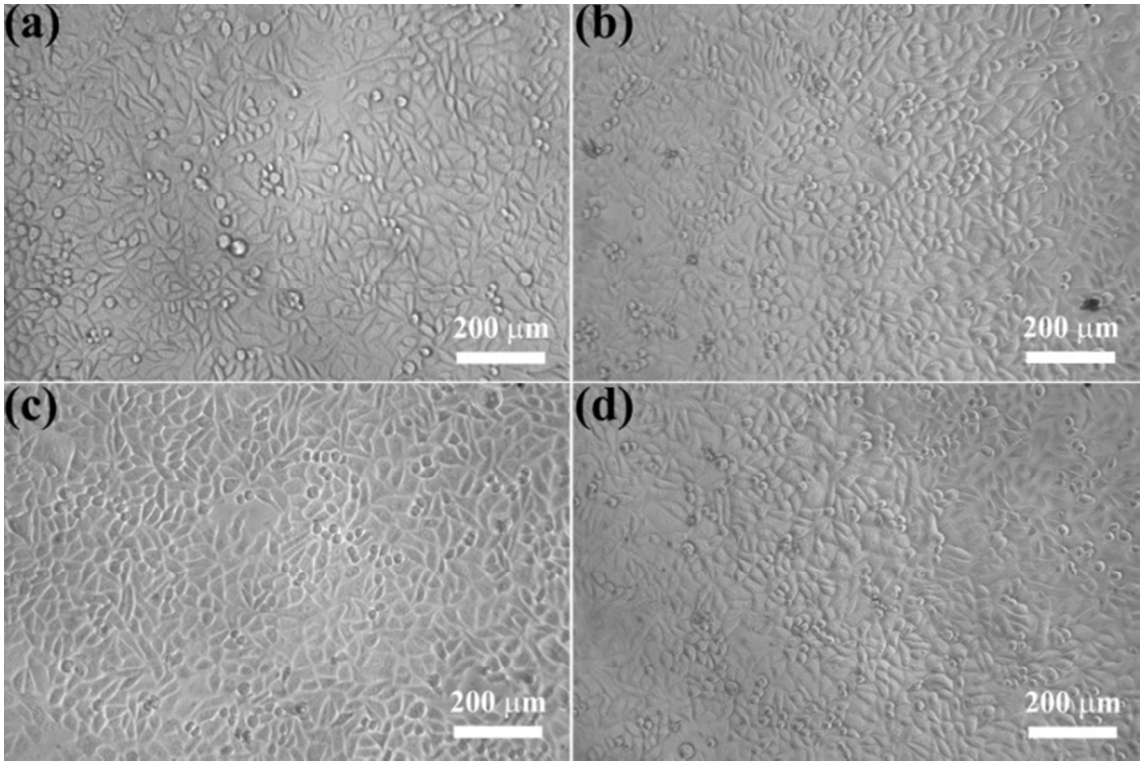

Figure S10. Optical micrographs of Hela cells after being treated with (a) 0, (b) 25, (c) 50 and (d) 100 μg/mL RH-GQDs for 24 h.

Reference:

1. Ju, S.-Y.; Kopcha, W. P.; Papadimitrakopoulos, F., Brightly Fluorescent Single-Walled Carbon Nanotubes via an Oxygen-Excluding Surfactant Organization. *Science* **2009,** *323* (5919), 1319-1323.